Preparation and Characterization of Dendrimer Layers on Poly(dimethylsiloxane) Films

Bong Jun Cha, Yong Soo Kang, and Jongok Won*

Center for Facilitated Transport Membranes, Korea Institute of Science and Technology, P.O. Box 131 Cheongryang, Seoul 130-650, Korea

Received March 12, 2001; Revised Manuscript Received June 15, 2001

ABSTRACT: Thin organic layers of polyamidoamine (PAMAM) dendrimers on poly(dimethylsiloxane) (PDMS) films were prepared, and their transport properties were evaluated. The surface of the PDMS film was plasma-modified either in air or in maleic anhydride (MAH) vapor. In the case of the MAH-plasma-treated surface, the majority of anhydride groups were maintained during the plasma treatment. Stable dendrimer layers were deposited by simple loading of amine-terminated PAMAM dendrimer solutions on the air-plasma-treated PDMS film to make PDMS−dendrimer membranes and were formed by reacting amine groups of the PAMAM dendrimers with anhydride groups on the MAH-plasma-treated surface to prepare PDMS−anhydride−dendrimer composite membranes. The dendrimer layers were characterized using XPS, ATR FT-IR spectrometry, and contact-angle and gas permeance measurements. Both PDMS−anhydride and PDMS−anhydride−dendrimer composite films showed facilitated transport of propylene when coordinated with silver salts. The propylene permeance and ideal separation factor over propane were 34 GPU and 340, respectively, at high silver loading.

Introduction

Dendrimers have received a great deal of attention because of their versatility in having surface functional groups that can be post-functionalized to highly ordered, ultrathin films. A variety of strategies has been developed for attaching dendrimers to the surface of a substrate, mainly metal surfaces. Approaches to thin film formation of dendritic molecules include the use of ionic and covalent bonding between adjacent layers.[1−7] For example, dendrimers have been immobilized onto an amine-functionalized silicon surface and subsequently complexed with Pt ions to make thin dendrimer films.[2] It has been found that protonation of amine-terminated dendrimers leads to adsorption on a hydrophilic silicon oxide surface.[2] Redox-active ferrocenyl dendrimers have been electrochemically deposited onto a Pt electrode.[4,5] Dendrimer mono- and multilayers on Au and hydroxylated Si-containing surfaces have also been studied.[6,7] Dendrimer-based thin films on an organic substrate have also been prepared.[8,9]

Here, we describe a simple method for the formation of dendritic thin layers on a polymeric matrix. This simple approach can be used as a general synthetic method for preparing functional thin films. Thin films of dendritic polymers offer interesting application possibilities, including uses as encapsulant coatings, redox ion channels, catalytic and biocompatible membranes, and adhesion promoters and inhibitors. These applications would benefit from dendritic thin films and coatings.

In this study, thin layers of amine-terminated Starburst (PAMAM) dendrimers were prepared on plasma-treated poly(dimethylsiloxane) (PDMS) substrates. The surface of the PDMS substrate was modified to enhance the adhesion between the dendrimer layer and the substrate surface by treatment with either air or maleic anhydride (MAH) plasma, as shown in Scheme 1. The dendritic thin films were characterized by ATR FT-IR spectrometry and XPS, and facilitated olefin transport through the composite membranes was investigated. The chemistry described here is simple for preparing highly functionalized nanocomposite membranes on polymeric matrixes without using any solvent. The strategy described here is also versatile and, therefore, has excellent potential for technological applications.

* To whom correspondence should be addressed. Tel.: +82-2-958-5287. Fax: +82-2-958-6869. E-mail: jwon@kist.re.kr.

Experimental Section

Materials. Poly(dimethylsiloxane) (PDMS; product SSP-M100, 130 μm thick) film as a polymeric substrate was purchased from Specialty Silicone Products, Inc. (Ballston Spa, NY). A 10% solution of fourth-generation amine-terminated poly(amidoamine) (PAMAM) dendrimer in methanol (D; Aldrich), silver tetrafluoroborate ($AgBF_4$, 99.0% purity; Aldrich), maleic anhydride (MAH; Junsei), and methanol (Merck, RPA) were purchased and used as received.

PDMS−Dendrimer (PDMS−D) Composite Films. Plasma treatment was carried out using a R300A radio frequency generator (Autoelectric, Seoul), operating at 13.56 MHz and 50 W. A PDMS 4×4 cm^2 film was soaked in boiling methanol at 65 °C for 3 h and then sonicated for 1 h, washed in pure methanol and deionized water several times to remove any impurities, and dried in a vacuum for 2 days. All substrates were used immediately after drying for composite layer formation. The PDMS film was glow-discharged in air for 1 min under a pressure of 0.02 Torr in a bell-jar-type reactor (6 cm radius × 11 cm depth). Inductively coupled plasma was generated by a circular coil connected to a radio frequency generator. Dendrimer in the concentration range of (3.1×10^{-9})−(3.1×10^{-11}) mol/cm^2 was cast onto the air-plasma-modified PDMS films by solution deposition. After being allowed to dry at room temperature, the samples were annealed in a 120 °C oven for 1 h.

PDMS−Anhydride−Dendrimer (PDMS−AH−D) Composite Films. Different amounts of MAH were placed in a plasma reactor with PDMS films to introduce succinic anhydride groups on the PDMS films. PAMAM dendrimers were subsequently reacted with succinic anhydrides on the MAH-plasma-treated surface of the PDMS film to make PDMS−AH−D composite membranes. The plasma treatment conditions and following treatment were the same as those for the

10.1021/ma0104276 CCC: $20.00
Published on Web 08/11/2001

Scheme 1

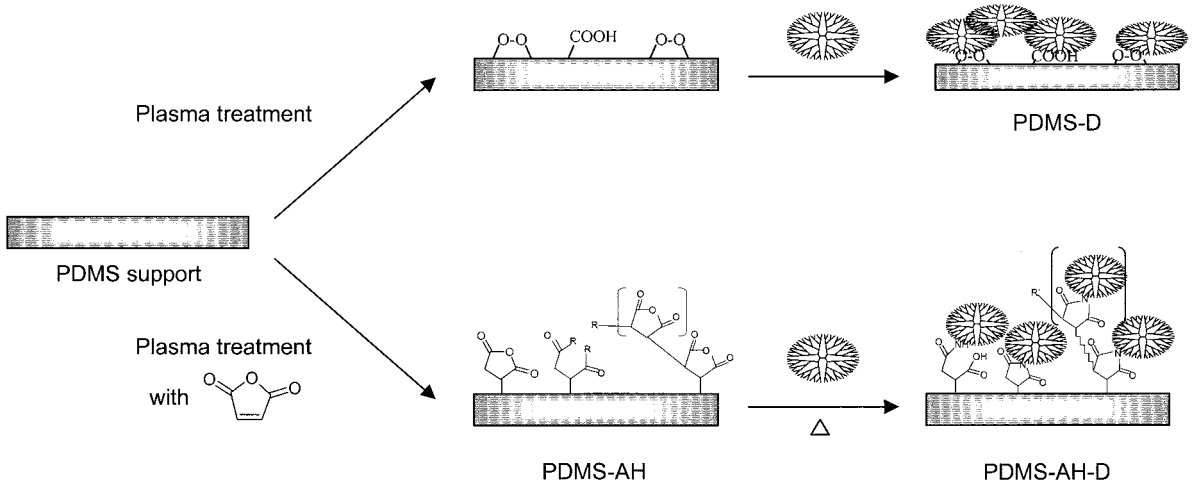

PDMS−D composite membrane. The PDMS−AH−D composite membrane was annealed at 120 °C for 1 h to induce the chemical reaction between the anhydrides and amines of dendrimers. All samples were then washed repeatedly with pure methanol and dried. Different amounts of $AgBF_4$ dissolved in methanol were loaded on the composite film and dried under vacuum. All samples were stored in a vacuum before characterization.

Characterization. FT-IR measurements were performed on a 6030 Galaxy Series FT-IR spectrometer (Mattson Instruments); 256 scans were signal-averaged at a resolution of 4 cm^{-1}. The ATR spectra were obtained using a KRS-5 prism with an incident angle of 45°. XPS measurements were carried out on a SSI 2803-S electron spectrometer (Surface Science Instruments) employing monochromated Al Kα (1486.7 eV) X-rays with an electron takeoff angle of 37°. The contact angles for all treated PDMS surfaces were determined using a contact angle meter (Tantec, model CAM-Micro). The contact angle of deionized water on surface-modified PDMS films was measured by the static drop method at room temperature. Each reported contact angle value is the average of at least six measurements. Propane (99.99%) and propylene (99.99%) were used for the permeation experiments, and pure gas permeation properties were measured by a soap-bubble flow meter. The feed pressure was maintained at 275.6 KPa, and the permeated pressure was atmospheric. The unit of gas permeance is the GPU, where 1 GPU = 1×10^{-6} cm^3(STP) cm^{-2} s^{-1} $cmHg^{-1}$.

Results and Discussion

PDMS−Dendrimer (PDMS−D) Films. It is widely accepted that surface oxidation occurs when air is introduced during plasma treatment. Surface oxidation includes the formation of several functional groups such as carboxylic acid, hydroxyl, ketone, and peroxide.[10] Figure 1 shows ATR FT-IR spectra for a pristine PDMS film, an air-plasma-treated PDMS film, and a PDMS−D composite films. PDMS−D composite films were prepared by casting dendrimer solutions onto an air-plasma-treated PDMS film, followed by drying. Hydrogen and ionic bonds between the dendrimer layer and the oxidized surface undoubtedly play a role in enhancing the stability of the PMDS-D membranes. Loading of PAMAM results in the appearance of the strong amide I and II bands at 1647 and 1559 cm^{-1}, respectively, which are characteristic for PAMAM (G4-NH_2) dendrimer.[3,11] This implies that the PAMAM molecules are adsorbed onto the air-plasma-treated surface to form thin, stable dendrimer layers, resulting in thin composite PDMS−D membranes.

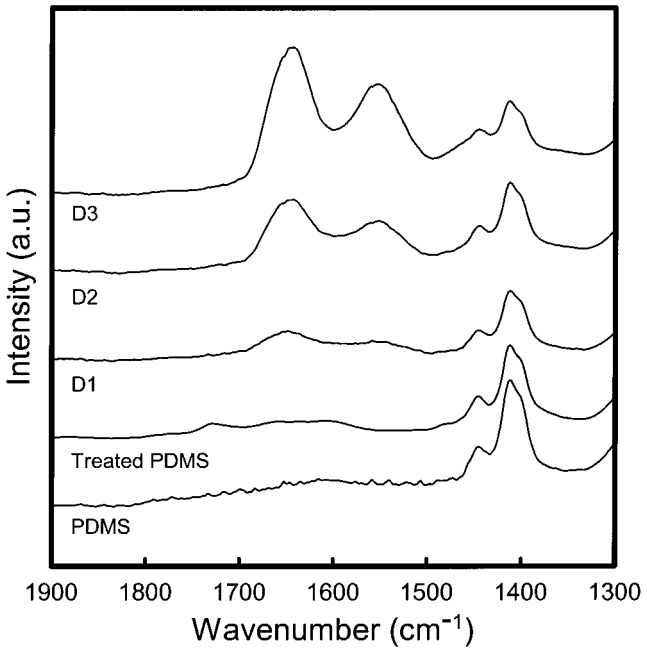

Figure 1. ATR FT-IR spectra of PDMS composite films. Spectra are shown for films of pristine PDMS; plasma-treated PDMS; and PDMS−D deposited with 10.5 (D1), 20.3 (D2), and 40 $\mu g/cm^2$ (D3) of dendrimers.

Table 1. Surface Characterization for PDMS−D Composite Films[a]

		XPS analysis					
	contact angle (°)	C (%)	O (%)	N (%)	Si (%)	surface coverage (%)	thickness, *d* (nm)
treated PDMS	85 ± 3	14.2	55.1		27.8		
D1	65 ± 3	43.0	19.8	0.7	11.4	3.5	0.1
D2	46 ± 1	54.7	20.3	11.8	13.3	59.8	2.2
D3	40 ± 2	62.1	21.8	16.1	−	82.2	−
PAMAM		65.5	14.9	19.6	−	−	

[a] The amounts of PAMAM dendrimer loaded on the plasma-treated PDMS films of D1, D2, and D3 are 10.5, 20.3, and 40 $\mu g/cm^2$, respectively.

The surface characteristics for the thin composite films containing PAMAM dendrimers are given in Table 1. The contact angle of pristine PDMS film is ca. 104° and that of air-plasma-treated PDMS film is 85°. The contact angle of PDMS−D films decreases monotonically

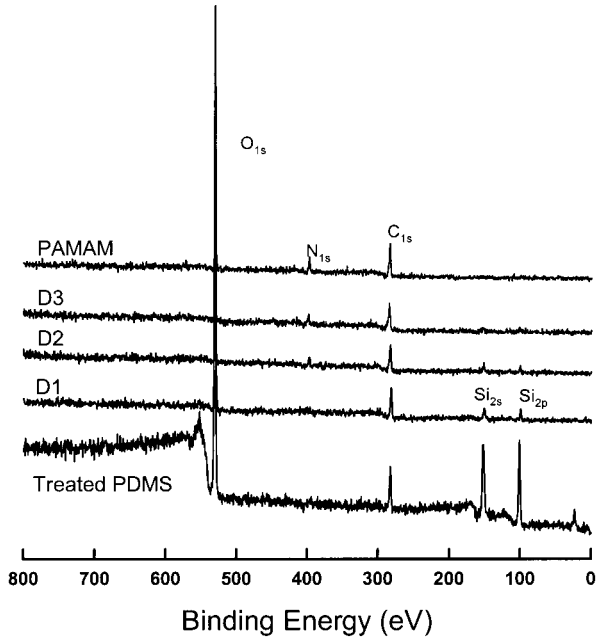

Figure 2. Wide-scan spectra for pristine and composite films containing dendrimers.

with dendrimer loading, thus suggesting that the surface becomes more hydrophilic.

Figure 2 shows wide-scan XPS spectra for the pristine PDMS and PDMS−D composite films. The N(1s) signal is observed in composite films containing PAMAM dendrimers because of the adsorption of PAMAM molecules, whereas it is not detected for the plasma-treated PDMS. Apparently, the Si(2s) and Si(2p) signals were decreased with increasing PAMAM dendrimer content. The spectrum in the D3 film shows no signals from Si(2s) and Si(2p), indicating that the surface of the PDMS substrate was mostly covered with dendrimers.

The atomic content from the XPS data is also given in Table 1. The XPS data show that the plasma-treated PDMS surface has 55 atom % of oxygen, which is higher than the oxygen content of the pristine PDMS film surface (48%). The amount of oxygen in the surface of the PDMS−D films decreases, whereas the amount of nitrogen increases, with increasing loading amount of the dendrimer.

To quantify the coverage of the dendrimer layer, we used the atomic content from the XPS data. Because the only source of nitrogen atomic signal is PAMAM, the surface coverage by dendrimer can be estimated simply by the ratio of the N(1s) signal observed for the PDMS−D composite films to that of PAMAM bulk, and the results are also shown in Table 1. The surface coverage increased with increasing dendrimer loading, which is consistent with the contact angle results, but incomplete coverage is shown even for a high loading of dendrimer (D3).

The PAMAM layer thickness, d, deposited on the substrate can be calculated from the relative intensities of the N(1s) signal using eq 1[12]

$$d = \lambda_{N1s} \sin\theta \ln(I_{N1s}^{\infty}/I_{N1s}^{\infty} - I_{N1s}) \qquad (1)$$

where I_{N1s} is the intensity of the N(1s) signal for the PAMAM layer, I_{N1s}^{∞} is that for an infinitely thick layer (in this case, PAMAM bulk solid), λ_{N1s} is the mean free path of the N(1s) electron in the PAMAM layer, and θ is the takeoff angle relative to the surface. The N(1s) photoelectron intensity is given by

$$I_{N1s} = I_{N1s}^{\infty}[1 - \exp(-d\lambda_{N1s} \sin\theta)] \qquad (2)$$

where λ_{N1s} can be calculated using the equation established for organic layers by Seah and Dench[12]

$$\lambda_{N1s} = \rho^{-1}(49E_k^{-2} + 0.11E_k^{0.5}) \qquad (3)$$

The value of E_k for the N(1s) photoelectron is calculated using

$$E_k = h\nu - E_b \qquad (4)$$

where $h\nu$ is the X-ray energy (1486.6 ev) and E_b is the N(1s) binding energy. Then, eq 3 can be simplified for electron kinetic energies greater than 150 eV to yield[12]

$$\lambda_{N1s} = \rho^{-1}0.11E_k^{0.5} \qquad (5)$$

where ρ is the density of the layer in g cm^{-3}. For PAMAM (G4-NH$_2$), ρ = 1.224 g cm^{-3}, and thus λ_{N1s} = 2.96 nm. The thicknesses of the dendrimer layers calculated using eq 1 are given in Table 1 and is in the range of 0.1−2.2 nm. The ultrathin dendrimer layer represents incomplete surface coverage.

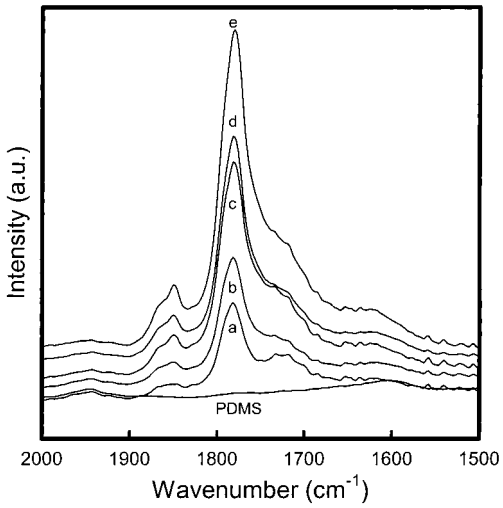

Figure 3. ATR FT-IR spectra of PDMS−AH films. Spectra are shown for pristine PDMS and PDMS composite films deposited with (a) 8.75×10^{-6}, (b) 1.75×10^{-5}, (c) 2.1×10^{-5}, (d) 2.5×10^{-5}, and (e) 3.3×10^{-5} g/cm^2 of maleic anhydride.

PDMS−Anhydride−Dendrimer (PDMS−AH−D) Films. PDMS films were MAH-plasma-treated to introduce reactive anhydride groups.[13,14] ATR FT-IR spectroscopy provides information on the surface of the MAH-modified PDMS film (PDMS−AH). Absorbance spectra of the pristine PDMS and PDMS−AH films with increasing loading of MAH are shown in Figure 3. The spectra of the PDMS−AH films showed three bands at 1850, 1782, and 1730 cm^{-1} that can be attributed to the asymmetric and symmetric anhydride C═O stretching modes of succinic anhydride and the C═O stretching modes of the carboxyl group resulting most likely from the ring-opening reaction of anhydride on the surface, respectively. The intensity of the 1782 cm^{-1} anhydride C═O stretching band is much stronger than that of the 1730 cm^{-1} band for ring-open carbonyls, meaning that the majority of the anhydride functionality is main-

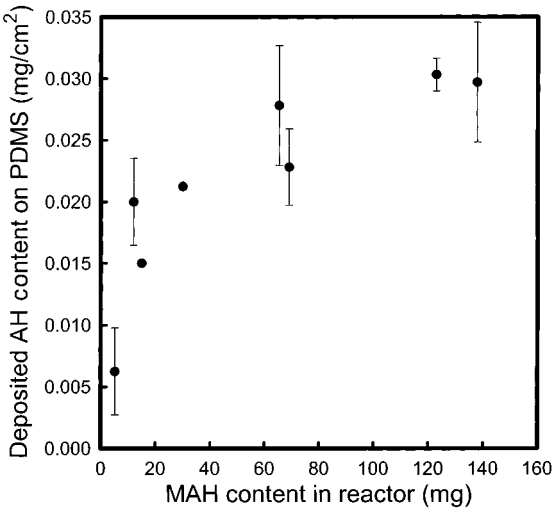

Figure 4. Deposited AH content with increasing maleic anhydride content in the reactor.

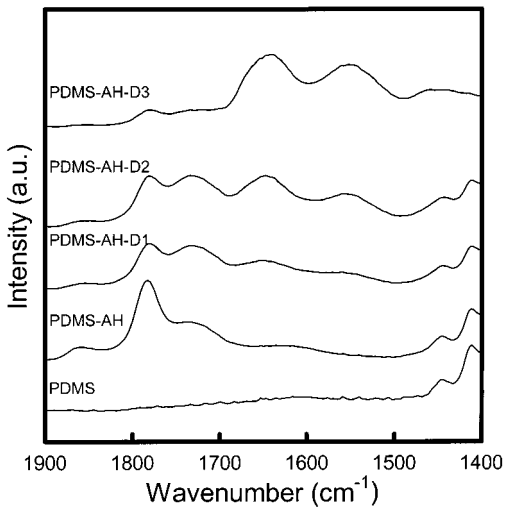

Figure 5. ATR FT-IR spectra of PDMS−AH composite films. Spectra are shown for films of (a) pristine PDMS; (b) PDMS−AH; and PDMS−AH−D deposited with (c) 3.1×10^{-11}, (d) 3.1×10^{-10}, and (e) 3.1×10^{-9} mol/cm^2 of dendrimers.

tained during plasma treatment. Figure 4 shows the amount of succinic anhydride deposited on the PDMS films with increasing loading of MAH in the plasma reactor. The deposited amount steeply increases until the amount of MAH in the reactor reaches 60 mg, and then it levels off.

To examine the effect of the experimental conditions on surface functionality, the concentration of maleic anhydride in the plasma reactor was varied. As shown in Figure 3, the succinic anhydride concentration increases with increasing concentration of maleic anhydride in the plasma reactor. Figure 3 also shows that both the 1782 cm^{-1} anhydride C═O and the 1730 cm^{-1} open C═O stretching modes increase simultaneously at similar rates, indicating that the relative concentration of the succinic anhydride is changed insignificantly with varying concentration of maleic anhydride in the plasma reactor. Therefore, it was found that succinic anhydrides are readily introduced onto the PDMS substrate when it is MAH-plasma-treated.

The succinic anhydride groups on the surface were subsequently reacted with the amine groups of PAMAM dendrimers to prepare PDMS−anhydride−dendrimer (PDMS−AH−D) composite films. ATR FT-IR spectra of the PDMS−AH−D composite films are shown in Figure 5. Two anhydride bands at 1850 and 1782 cm^{-1} for the PDMS−AH−D composite films decreased with increasing concentration of dendrimer solution, whereas two bands for amides at 1640 and 1550 cm^{-1} increased. This strongly suggests that some PAMAM dendrimer molecules reacted with amines on the substrate to make composite membranes. The chemistry used in the present work was developed by Crooks and Bergbreiter and their co-workers.[7,8,15,16] According to the results of Zhao et al.,[8] the reaction between amines and anhydrides gives amic acids, which are subsequently transformed to imides by heat treatment at 120 °C, as confirmed by IR spectroscopy. It was stated that transamidation and retro-Michael reactions along with imide formation are very likely to occur in bulk-phase reactions during the heat treatment at 120 °C.[8] In the present work, a broad peak at around 1710 cm^{-1} for imide appeared in the PDMS−AH−D1 membrane spectrum although the IR spectra did not provide clear evidence for such intradendrimer reactions. This could be mainly due to the low concentration of reaction adducts. Therefore, the dendrimer layer is linked covalently to the substrate film, resulting in thin PDMS−AH−D composite membranes.

Table 2. Propane Permeance of PDMS−D Composite Films

amount of PAMAM loaded (μg/cm^2)	permeance (GPU[a])
0	53
10.5	58
20.3	44
40.0	46
60.0	32

[a] 1 GPU = 1×10^{-6} cm^3(STP) cm^{-2} s^{-1} cmHg^{-1}.

Gas Transport Behavior. Table 2 shows the change in propane permeance of PDMS−D composite films with increasing loading amounts of PAMAM dendrimers. When a small amount of PAMAM dendrimer is loaded, the permeance of propane hardly changes because of the low coverage of the surface, but it decreases with increasing amounts of loaded dendrimer. The decreased permeance implies that the permeance of the dendrimer layer is lower than that of PDMS. The dendrimer layer would have the maximum effect on permeance as a uniform layer, which could not exceed 0.6 μm for the maximum loading of 60 μg/cm^2. This is obviously negligible compared to the value for the pristine PDMS ($\sim$130 μm), and thus, the effect of film thickness on gas permeance would be negligible in this experimental range. In addition, we have shown that the dendrimer layer is of nonuniform thickness, which only argues for an even lower permeance of dendrimer layer.

The pure propane and propylene permeances of the PDMS−AH films as functions of the inverse amount of deposition are shown in Figure 6. The permeances of all MAH-modified PDMS films were lower than that of the pristine PDMS films, which is ca. 100 GPU. The permeance shows a linear relation with the inverse of the anhydride deposition amount on the PDMS films. Under the assumption that the deposited amount of anhydride is linearly correlated with the thickness of the modified layer, the linear decrease of permeance means that permeance through the anhydride layer is the rate-determining step. These results are reasonable in the view of plasma polymerization.[14]

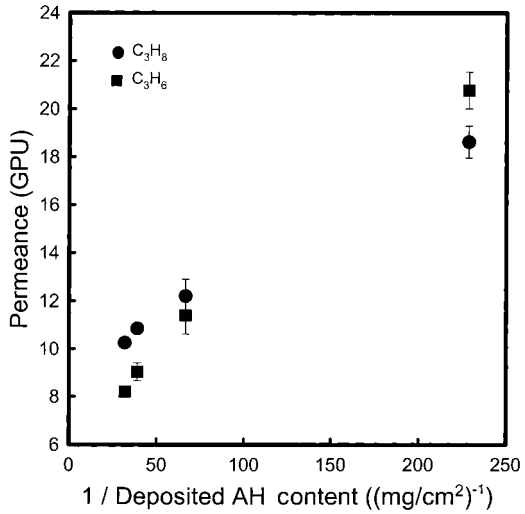

Figure 6. Gas permeance dependence on the amount of anhydride loaded on PDMS films.

Table 3. Gas Permeance of PDMS−AH Composite Films with $AgBF_4$ Content

AH[a] (mg/cm²)	$AgBF_4$ ($\times10^{-6}$ mol/cm²)	[Ag]/[AH][b] (mole ratio)	propylene (GPU[c])	propane (GPU)	ideal separation factor
0.025	–	–	9	11	0.82
0.029	0.32	1.07	28	6.5	4.3
0.025	1.2	4.57	21	2.6	8.1
0.025	2.6	10.11	5.7	<0.1[c]	>57

[a] The amount of MAH loaded in the plasma reactor was 80 mg. [b] Weight ratio of silver salt to molecular weight of anhydride monomer. [c] 1 GPU = 1×10^{-6} cm³(STP) cm^{-2} s^{-1} cmHg^{-1}. [d] The permeance of propane was not detected as it was below the practical lower limit of the bubble flow meter.

It has been understood that low-lattice-energy silver salts confined to polymers containing polar groups such as oxygen, nitrogen, and sulfur form reversible complexes with olefin molecules and that such reversible and specific interactions of silver ions with olefin molecules leads to carrier-mediated transport in addition to normal Fickian transport in the solid[17−24] and liquid states.[25−29]

PDMS−AH Membrane Complexed with $AgBF_4$. The effect of silver salt concentration on olefin/paraffin separation was investigated through a PDMS−AH membrane complexed with $AgBF_4$. The gas permeances through the MAH-modified PDMS films with increasing loadings of $AgBF_4$ are shown in Table 3. The propane permeance through the film decreased with increasing silver ion content. Propane is unable to form complexes with silver ions and permeates only through Fickian transport. The dissolved silver salts induce a decrease in the mobility of polymeric chains, and this reduced mobility hinders the gas permeance.[30] The reduced mobility is due to the role of ion as a cross-linking point, which was confirmed by the increasing glass transition temperature for other silver-coordinated systems.[30] Therefore, the decreasing mobility of the polymer chain with increasing loading of salt would affect the gas transport behavior. Another possible explanation for the decreasing permeance is that, when the silver salt is introduced at a level greater than the solubility limit of the MAH-modified layer, the excess silver salt might form a layer on top of the surface. It is well-known that there are free ions, contact ion pairs, and higher ion aggregates in a number of polymer electrolytes at higher salt concentrations.[31−36] Excess amounts of loaded salt would act as a barrier for gas transport, leading to a significantly decreased gas permeance. Meanwhile, the propylene permeance through PDMS−AH films increased from ca. 9 to ca. 28 GPU when the mole ratio of [Ag^+] to [AH] was close to 1. The ideal separation factor for propylene/propane, defined as the ratio of the permeance of propylene to that of propane, is ca. 4. Having a selectivity greater than 1 implies that silver ions dissolved by the anhydride moieties, especially carbonyl groups on the surface of PDMS, act as propylene carriers and lead to facilitated propylene transport.[17−22] It has also been shown that coordination of silver salts with carbonyl groups in poly(vinyl methyl ketone) results in facilitated propylene transport.[37]

Table 4. Gas Permeance of PDMS Composite Membranes with Silver Salts

	PDMS−AH[a]−D[b]		
$AgBF_4$ ($\times10^{-6}$ mol/cm²)	propylene (GPU[c])	propane (GPU)	ideal separation factor
0	5.5	5.3	1.0
1.6	17	6.9	2.5
3.1	17	<0.1[d]	>170
16	34	<0.1[d]	>340

[a] The amount of AH loaded was determined to be 0.03 mg/cm². [b] The amount of PAMAM dendrimer loaded was 10.5 μg/cm². [c] 1 GPU = 1×10^{-6} cm³(STP) cm^{-2} s^{-1} cmHg^{-1}. [d] The permeability of propane is assumed to be <0.1 GPU because it was not detected, being below the practical lower limit of the bubble flow meter.

PDMS−AH−D Membrane Complexed with $AgBF_4$. According to the theory of facilitated transport, a higher carrier concentration results in enhanced facilitated transport.[38] A high carrier concentration can be achieved by introducing good macromolecular solvents such as dendrimers for silver salts. In this respect, PAMAM dendrimers containing many carbonyl functional groups can be used to provide extra sites for silver coordination.

The propylene permeances through the dendrimer composite membranes with increasing amounts of $AgBF_4$ are shown in Table 4. Because of the unknown quantity of functional groups in the dendrimer layer, the mole ratio of silver to functional groups was not readily quantified, although we expected that the amount of loaded silver salts were in excess. The propane permeances through both PDMS−D (Table 2) and PDMS−AH−D (Table 4) membranes decreased with increasing salt concentration because of the cross-linking effect of silver salts, as described previously, but the decrease was more significant for the former than for the latter. In comparison, the propylene permeance through PDMS−AH−D membranes increased from 5 to 34 GPU with increasing silver ion content. The propylene permeance through the PDMS−AH−D membrane is much higher than that through the PDMS−AH membrane, whereas the propane permeance did not change significantly. Therefore, the ideal separation factor for propylene/propane is more than 340 at high silver concentration.[39] The enhanced propylene permeance through the PDMS−AH−D membrane compared to that through the PDMS−AH membrane seems to be primarily due to the extra loading capability of silver salts by the dendrimer molecules.

Summary

Thin dendrimer layers on polymer films were prepared and characterized by XPS, ATR FT-IR spectroscopy, and gas transport measurements. The surface of the PDMS films was modified in air and in the presence of maleic anhydride by a simple plasma technique. In the case of the MAH plasma treatment, the chemical composition of the surface was mostly succinic anhydrides, which were subsequently allowed to react with the amine groups in PAMAM dendrimers. It was found that the dendrimer layer reduced the gas permeance. Facilitated olefin transport through the composite films when complexed with silver salts was investigated. For the PDMS−AH−D films, the propylene permeance and its ideal separation factor over propane increased from ca. 5 to 34 GPU and from ca. 1 to 340, respectively, with increasing silver salt concentration. This excellent facilitated transport behavior can predominantly be attributed to the large amount of silver ions that can be loaded on PAMAM dendrimers containing many carbonyls, which interact with propylene reversibly and specifically.

Acknowledgment. We are grateful for financial support from the Ministry of Science and Technology of Korea through the Creative Research Initiatives Program.

References and Notes

(1) Tsukruk, V. V.; Rinderspacher, F.; Bliznyuk, V. N. *Langmuir* **1997**, *13*, 2171.
(2) Watanabe, S.; Regen, S. I. *J. Am. Chem. Soc.* **1994**, *116*, 8855.
(3) Tokuhisa, H.; Zhao, M.; Baker, L.; Phan, V. T.; Dermody, D. L.; Garcia, M. E.; Peez, R. F.; Crooks, R. M.; Mayer, T. M. *J. Am. Chem. Soc.* **1998**, *120*, 4492.
(4) Alonso, B.; Moran, M.; Casado, C. M.; Lohele, F.; Losada, J.; Cuadrado, I. *Chem. Mater.* **1995**, *7*, 1440.
(5) Takada, K.; Diaz, D. J.; Abruna, H. D.; Cuadrado, I.; Casado, C.; Alonso, B.; Moran, M.; Losada, J. *J. Am. Chem. Soc.* **1997**, *119*, 10763.
(6) Wells, M.; Crooks, R. M. *J. Am. Chem. Soc.* **1996**, *118*, 3988.
(7) Liu, Y.; Bruening, M. L.; Bergbreiter, D. E.; Crooks, R. M. *Angew. Chem., Int. Ed. Engl.* **1997**, *36*, 2114.
(8) Zhao, M.; Liu, Y.; Crooks, R. M.; Bergbreiter, D. E. *J. Am. Chem. Soc.* **1999**, *121*, 923.
(9) Bergbreiter, D. E.; Crooks, R. M.; Dermody, D. L.; Jones, S. J.; Liu, Y.; Franchina, J. G.; Bruening, M. L.; Zhou, Y.; Zhao, M. *Polym Mater. Sci. Eng.* **1998**, *79*, 444.
(10) Yasuda, H. *J. Macromol. Sci.-Chem.* **1976** *A10*, 383.
(11) Garcia, M. E.; Baker, L. A.; Crooks, R. M. *Anal. Chem.* **1999**, *71*, 256.
(12) Chan, C. M. *Polymer Surface Modification and Characterization*; Hanser Publishing: München, Germany, 1994; Chapter 3.
(13) Gaboury, S. R.; Urban, M. W. *Langmuir* **1993**, *9*, 3225; **1994**, *10*, 2289.
(14) Ryan, M. E.; Hynes, A. M.; Badyal, J. P. S. *Chem. Mater.* **1996**, *8*, 37.
(15) Liu, Y.; Zhao, M.; Bergbreiter, D. E.; Crooks, R. M. *J. Am. Chem. Soc.* **1997**, 119, 8720.
(16) Bergbreiter, D. E.; Franchina, J. G.; Kabza, K. *Macromolecules* **1999**, *32*, 4953.
(17) Yoon, Y. S.; Won, J.; Kang, Y. S. *Macromolecules* **2000**, *33*, 3185.
(18) Hong, S. U.; Jin, J. H.; Won, J. Kang, Y. S. *Adv. Mat.* **2000**, *12*, 968.
(19) Park, Y. S.; Won, J.; Kang, Y. S**.** *Langmuir* **2000**, *16*, 9662.
(20) Kim, Y. H.; Ryu, J. H.; Bae, J. Y.; Kang, Y. S.; Kim, H. S. *Chem. Commun.* **2000**, 195−196.
(21) Jin, J, H.; Hong, S. U.; Kang, Y. S. *Macromolecules* **2000**, *33*, 4932.
(22) Park, Y. S.; Won, J.; Kang, Y. S. *J. Membrane Sci.* **2001**, *183*, 163.
(23) Pinnau, I.; Toy, L. G.; Sunderrajan, S.; Freeman, B. D. *Polym. Mater. Sci. Eng.* **1997**, *79*, 269.
(24) Pinnau, I.; Toy, L. G.; Casillas, C. U.S. Patent 5,670,051, 1997.
(25) Yang, J. S.; Hsiue, G. H. *J. Membr. Sci***. 1996**, *111*, 27.
(26) Yang, J. S.; Hsiue, G. H. *J. Membr. Sci.* **1996**, *120*, 69.
(27) Yamaguchi, T.; Baertsch, C.; Koval, C. A.; Noble, R. D.; Bowman, C. N. *J. Membr. Sci.* **1996**, *117*, 151.
(28) Ho, W. S.; Dalrtmple, D. C. *J. Membr. Sci.* **1994**, *91*, 13.
(29) LeBlanc, O. H.; Ward, W. J., III; Matson, S. L.; Kimura, S. G. *J. Membr. Sci.* **1980**, *6*, 339.
(30) Kim, J. Y.; Hong, S. U.; Won, J.; Kang, Y. S. *Macromolecules* **2000**, *33*, 3161.
(31) Teeters, D.; Frech, R. *Solid State Ionics* **1986**, *18/19*, 271.
(32) Frech, R.; Manning, J.; Black, B. *Solid State Ionics* **1988**, *28/30*, 954.
(33) Dissanayake, M. A. K. L.; Frech, R. *Macromolecules* **1995**, *28*, 5312.
(34) Papke, B. L.; Ratner, M. A.; Shriver, D. F. *J. Phys. Chem.* **1981**, *42*, 493.
(35) Huang, W.; Frech, R.; Wheeler, R. A. *J. Phys. Chem.* **1994**, *98*, 100.
(36) Papke, B. L.; Dupon, R.; Ratner, M. A.; Shriver, D. F. *Solid State Ionics* **1981**, *5*, 685.
(37) Kim, H. S.; Ryu, J. H.; Kim, H.; Ahn, B. S.; Kang, Y. S. *Chem. Commun.* **2000**, 1261.
(38) Kang, Y. S.; Hong, J. M.; Kim, U. Y.; Jang, J. *J. Membr. Sci***. 1996**, 109, 149.
(39) We assumed that the permeability of propane is 0.1 GPU because it was not detected as it was below the practical lower limit of the bubble flow meter.

MA0104276